

Sagnac-interferometer-based characterization of spatial light modulators

Jian Wei Tay,¹ Michael A. Taylor,¹ and Warwick P. Bowen^{1,2,*}

¹Jack Dodd Centre for Quantum Science, Physics Department, Otago University, P.O. Box 56, Dunedin, New Zealand

²School of Physics and Mathematics, University of Queensland, Brisbane 4072, Australia

*Corresponding author: wbowen@physics.uq.edu.au

Received 1 December 2008; revised 18 February 2009; accepted 26 March 2009; posted 27 March 2009 (Doc. ID 104670); published 14 April 2009

A method for characterizing the phase response of spatial light modulators (SLMs) by using a Sagnac interferometer is proposed and demonstrated. The method represents an improvement over conventional diffraction-based or interferometric techniques by providing a simple and accurate phase measurement while taking advantage of the inherent phase stability of a Sagnac interferometer. As a demonstration, the phase response of a commercial liquid crystal on a silicon SLM is characterized and then linearized by using a programmable lookup table. The transverse phase profile over the SLM surface is also measured. © 2009 Optical Society of America

OCIS codes: 120.3180, 120.5050, 230.3720, 230.6120.

1. Introduction

Spatial light modulators (SLMs) are becoming more commonplace both in the optics laboratory and elsewhere. Their use extends from optical pulse shaping [1,2], computer generated holography [3–5], optical metrology [6,7], generating programmable lenses or diffractive optical elements [8–10], and optical tweezers [11,12] to medical applications in optical coherence tomography [13] and even atom optics [14,15]. Such a modulator is capable of modifying the phase of light, allowing the spatial mode properties to be changed almost arbitrarily.

It is important to characterize the phase shift imparted by the SLM as a function of steerable parameters such as voltage, and due to manufacturing imperfections such as silicon backplane curvature, before the SLM is used in an experiment. This *phase response* is determined most commonly by using diffraction-based techniques [16–18] or interferometry [3,19–22]. Diffraction-based techniques use the SLM configured as a diffractive grating and measure

the distribution of the light in the far field by using a CCD camera. An advantage of diffraction-based methods over interferometers is that they naturally characterize the phase difference between spatially separate components of the SLM; i.e., they do not require a stable reference. However these techniques usually involve a complex theoretical model that contains several unknown parameters to match the measured data. These parameters need to be found by collecting large sets of data with different configurations (such as grating depth) or prior knowledge such as pixel-to-pixel phase variations. Therefore the disadvantage of these techniques include ambiguities due to the underdefined nature of these parameters, the large number of measurements needed to obtain them, and the limited bandwidth due to the requirement of using a CCD. Many methods also involve measuring the intensity in the zeroth diffraction order, which adds to the ambiguity, as this is strongly influenced by the “dead zones,” or gaps between pixels [18].

Interferometer-based measurements overcome most of these limitations by measuring the phase difference directly between the reference and the signal arms of an interferometer. Measurements made are

0003-6935/09/122236-07\$15.00/0

© 2009 Optical Society of America

simple to interpret, are unambiguous, and allow fast photodiode-based detectors to be used. However, most interferometers are disadvantaged by environmental factors affecting the optical path length between the two arms, such as air turbulence, mechanical vibrations, and drift. A stable reference is crucial for precision, as the phase measurements are made relative to this. Interferometers also tend to require elements such as piezoelectric transducers and active control electronics to maintain path length or provide a phase reference.

We present here a novel way of measuring the phase response of an SLM by using a Sagnac interferometer. This method combines the advantages of interferometric and diffraction-based schemes. In a Sagnac interferometer, an input field is split into two counterpropagating fields traveling along the same optical path, which are then recombined at a beam splitter. In typical use, all the light traveling in a Sagnac interferometer is returned along the path from which it entered. However, we show that if a phase shift about the normal of the interferometer plane is introduced, light is coupled out the dark port and can then be detected. This property allows us to use a Sagnac interferometer to characterize the phase response of an SLM with none of the drawbacks from the methods mentioned above. The method proposed is simple, is quick, and does not need an external reference [21,22]. As the beams travel the same path within it, this type of interferometer is also insensitive to factors that change the optical path length, giving a strong advantage over other forms of interferometry.

This method builds on results from the quantum optics community where Mach–Zehnder interferometers are utilized to spatially filter [23] or combine beams [24,25] with asymmetric transverse beam profiles. Sagnac interferometers are renowned for enabling ultraprecise rotation measurements; this paper extends their sensing capabilities to the characterization of spatially structured phase elements.

As a demonstration we characterize a commercial liquid crystal on silicon SLM and linearize its response with steerable beam parameter, using a programmable lookup table (LUT). The use of an interferometric technique with high bandwidth detection enabled the fast flicker due to the electrical characteristics of the device to be detected and quantified. The liquid crystal within an SLM in general varies in thickness, giving rise to a transversely varying phase response. Diffraction-based methods are typically unable to measure this transverse profile. Here we use our method to experimentally characterize the transverse phase profile of the SLM surface.

2. Theoretical Analysis

We begin by describing the Sagnac interferometer as shown in Fig. 1. We have defined the \hat{z} axis in the direction of propagation of the laser beam, \hat{y} as normal to the plane of the interferometer, and $\hat{x} = \hat{y} \times \hat{z}$. As we will see in the theory that follows, Sagnac in-

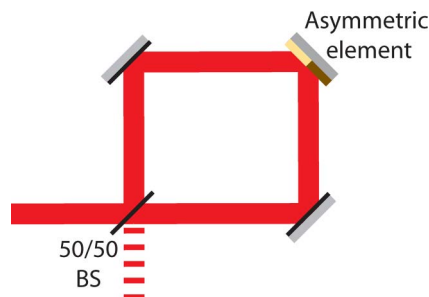


Fig. 1. (Color online) Schematic of a three-mirror Sagnac interferometer. One of the mirrors has been replaced with a transversely asymmetric element that introduces a phase shift between its two halves. BS, beam splitter.

terferometers with an odd number of mirrors are sensitive to phase variations that are asymmetric about the normal of the interferometer plane, \hat{y} .

The beam entering the Sagnac via the 50/50 beam splitter can be described as

$$E_{\text{in}}(x,y) = AU(x,y),$$

where A is the input field amplitude and $U(x,y)$ is its normalized transverse field profile with $\int \int_{-\infty}^{\infty} U(x,y) dx dy = 1$.

One of the mirrors is replaced with a transversely asymmetric phase element, such as an SLM, which imparts a spatially dependent phase shift, $\phi(x,y)$, to the field. The beam entering the interferometer gets split into two paths, one traveling clockwise and the other anticlockwise through the interferometer. For each field, reflection off a mirror causes its transverse profile to be reflected about the \hat{y} axis. Since the clockwise propagating field experiences an additional reflection after the phase element, the phase encoded on it is reflected an additional time. In the ideal case where we have perfect spatial mode overlap, the two fields after complete propagation through the interferometer are found to be described by

$$E_{\text{C}}(x,y) = \frac{1}{\sqrt{2}}AU(-x,y)e^{ikL}e^{i\phi(-x,y)},$$

$$E_{\text{A}}(x,y) = \frac{1}{\sqrt{2}}AU(-x,y)e^{ikL}e^{i\phi(x,y)},$$

where the field traveling clockwise has been marked with subscript C, the field traveling anticlockwise with subscript A, k is the wave vector, and L is the round-trip length of the interferometer. Since both beams travel along the same path, the Sagnac interferometer is unaffected by the mechanical instability, drift, or local air turbulence that plagues most interferometer setups.

The two fields recombine at the beam splitter and interfere, with the field at the dark port of the interferometer given by

$$\begin{aligned}
E_{\text{out}}(x,y) &= \frac{1}{\sqrt{2}}[E_C(x,y) - E_A(x,y)] \\
&= \frac{1}{\sqrt{2}}AU(-x,y)e^{ikL} \left[e^{i\phi(-x,y)} - e^{i\phi(x,y)} \right] \\
&= \frac{1}{\sqrt{2}}E_{\text{in}}(-x,y)e^{ikL} \left[e^{i\phi(-x,y)} - e^{i\phi(x,y)} \right]. \quad (1)
\end{aligned}$$

The intensity at the dark port of the interferometer, $I_{\text{out}}(x,y)$, is then

$$\begin{aligned}
I_{\text{out}}(x,y) &= \frac{c\epsilon_0}{2}|E_{\text{out}}(x,y)|^2 \\
&= \frac{1}{2}I_{\text{in}}(-x,y)[1 - \cos \Delta\phi(x,y)], \quad (2)
\end{aligned}$$

where c is the speed of light, ϵ_0 is the permittivity of free space, $I_{\text{in}}(x,y)$ is the intensity of the light entering the interferometer, and $\Delta\phi(x,y)$ is the phase difference between two points spaced equally apart about the \hat{y} axis, i.e., $\Delta\phi(x,y) = \phi(x,y) - \phi(-x,y)$. We see that the output light intensity from a Sagnac interferometer at position (x,y) is dependent on the difference in phase between two corresponding points on the phase element at positions (x,y) and $(-x,y)$. The measurement is therefore self-referenced, similar to measurements done by using diffraction-based methods, and there is no need for a reference arm as in other interferometer-based methods. If no asymmetric phase shift were present, i.e., $\phi(x,y) = \phi(-x,y)$, there would be complete destructive interference at the dark port as expected and $I_{\text{out}}(x,y) = 0$.

Using Eq. (2) we can directly determine the phase difference (modulo 2π) as a ratio of input and output intensity, given by

$$\Delta\phi(x,y) = \cos^{-1} \left[1 - 2 \frac{I_{\text{out}}(x,y)}{I_{\text{in}}(-x,y)} \right].$$

This equation provides a clear interpretation that allows us to derive the phase response of an SLM in a simple manner compared with diffraction-based methods.

In practice, the signal measured is the power P_{out} exiting the dark port and impinging on a detector of area A ,

$$\begin{aligned}
P_{\text{out}} &= \int_A I_{\text{out}}(x,y) dA \\
&= \frac{1}{2} \int_A I_{\text{in}}(-x,y) [1 - \cos \Delta\phi(x,y)] dA \\
&= \frac{1}{2} P_{\text{in}} [1 - \cos \bar{\Delta\phi}], \quad (3)
\end{aligned}$$

where the power entering the Sagnac interferometer $P_{\text{in}} = \int_A I_{\text{in}}(x,y) dA = \int_A I_{\text{in}}(-x,y) dA$ and $\Delta\phi(x,y) = \Delta\phi$, which is assumed to be constant over the area of the detector. This assumption is valid for a small

enough detector and is justified in our case by the experimentally observed phase fluctuations across the entire SLM of 8% (see Fig. 7 below). $\Delta\phi$ can now be interpreted as the averaged phase difference between two sections of the SLM surface located symmetrically on either side of the \hat{y} axis. Equation (3) can be rearranged for $\Delta\phi$ to give

$$\bar{\Delta\phi} = \cos^{-1} \left[1 - 2 \frac{P_{\text{out}}}{P_{\text{in}}} \right]. \quad (4)$$

In nonideal cases where there is imperfect spatial overlap between the clockwise and counterclockwise propagating fields, it is relatively straightforward to show that Eq. (4) becomes

$$\bar{\Delta\phi} = \cos^{-1} \left[\frac{1}{\text{VIS}} \left(1 - 2 \frac{P_{\text{out}}}{P_{\text{in}}} \right) \right], \quad (5)$$

where VIS is the interferometer visibility defined as

$$\text{VIS} = \frac{P_{\text{max}} - P_{\text{min}}}{P_{\text{max}} + P_{\text{min}}},$$

with P_{max} and P_{min} being the maximum and minimum powers observed at the dark port as $\Delta\phi$ is swept through 2π .

3. Phase Response Characterization

A. Experimental Setup

We demonstrate the phase characterization capabilities of the Sagnac interferometer with a commercial SLM (a Holoeye HEO-1080P liquid crystal on silicon display having a resolution of 1920×1080 pixels) with the experimental setup as shown in Fig. 2. We used an Innolight Prometheus Nd:YAG laser operating at 1064 nm with an optical isolator to prevent backscattered and backreflected light reentering the laser. The beam is expanded and collimated by appropriate lenses before entering the Sagnac. The Sagnac itself is constructed from a 50/50 beam splitter

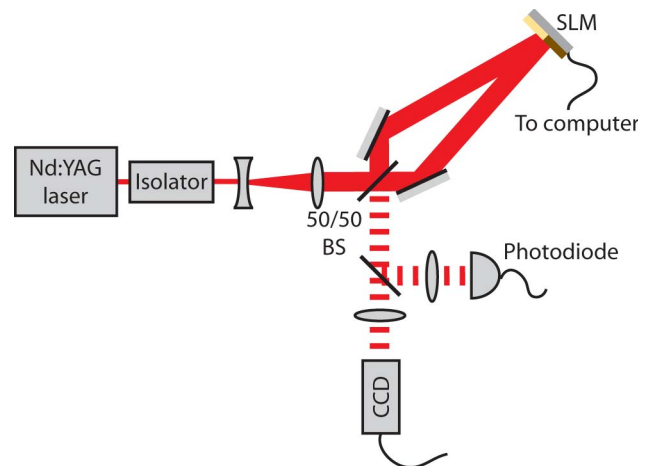


Fig. 2. (Color online) Schematic of experimental setup. SLM, spatial light modulator; BS, beam splitter; CCD, CCD camera.

ter, two mirrors, and the SLM. The interferometer is aligned such that the beams arrive at near-normal incidence on the SLM to avoid higher-order diffraction off the dead zones. As the beams travel along the same path, the Sagnac interferometer is insensitive to path length variations and does not require any piezo actuators or other path length compensations. The mode overlap between counterpropagating fields was optimized by minimizing the intensity at the dark port of the interferometer with no signal applied to the SLM.

The SLM is connected via DVI cable to a computer and acts as a second screen. The steerable parameter here is the gray-scale value on the screen which corresponds to a voltage applied across the corresponding pixel on the SLM. This voltage causes the crystal to change in optical depth, imparting a phase shift upon reflection of light off its active surface. According to the manufacturer's specifications, when fully on (gray-scale value of 255) the SLM induces a near- 2π phase shift for an optical wavelength of 1064 nm. The gray scale to voltage conversion is controlled by an internally programmable LUT. To vary the phase shift, a movie is used that holds the left half of the screen at zero gray-scale value while transitioning the right half from zero (black) to 255 (white). The movie was made at 4 frames/s, with the gray-scale value changed for each frame. The phase response of the right half of the SLM could then be characterized relative to the fixed left half. To characterize the left half, a second movie with the right half held fixed and the left half varied can be used, thus enabling full phase response characterization with just two measurements, as opposed to several needed in diffraction-based methods.

The phase response measurements in the following sections are made, as shown in the theory, between two sections of the SLM symmetrically located on either side of the \hat{y} axis. This allows measurements to be self-referenced, removing the need for precision optics required by conventional interferometers to produce a flat reference beam. Any inherent phase difference between the two sections, for example due to differences in polishing during manufacturing, will cause the gray-scale value at which the minimum dark port power occurs to be nonzero (see, for example, Fig. 6 below). This phase difference can then be immediately characterized by using Eq. (5).

B. Characterization of the Average Phase Response

To characterize the average phase response of the SLM, the beam exiting the dark port of the Sagnac was focused onto a high-bandwidth Thorlabs PDA36A photodetector. The movie was played, causing a temporal variation in the optical thickness of the right half of the SLM, and a consequential variation in the dark port power. The output intensity at the dark port as a function of time is shown in Fig. 3, part I. Since the entire output field was incident on the photodetector, Eq. (5) provides the average phase

difference between the optically illuminated parts of the two halves of the SLM, where P_{\min} and P_{\max} were determined directly from the averaged trace in the figure, and the power entering the interferometer was determined *in situ* as $P_{\text{in}} = P_{\max} + P_{\min}$. As can be seen from both Eq. (5) and Fig. 3, there is a turning point in P_{out} around the phase difference $\Delta\phi = \pi$, leading to an ambiguity in the determined phase difference around this point. To correct for this phase wraparound, we use P_{\max} to identify the point at which the phase difference is equal to π . As we are confident that the phase difference continues to increase after this point, the data is adjusted accordingly. The resulting phase response is shown in Fig. 3, part II. Note that the phase response of an arbitrary region of the SLM can be determined by choosing to vary the gray-scale value of that region only. This is an important aspect of the Sagnac characterization technique that provides additional flexibility.

Because of the high bandwidth of our detection system, the noise on the intensity measurements

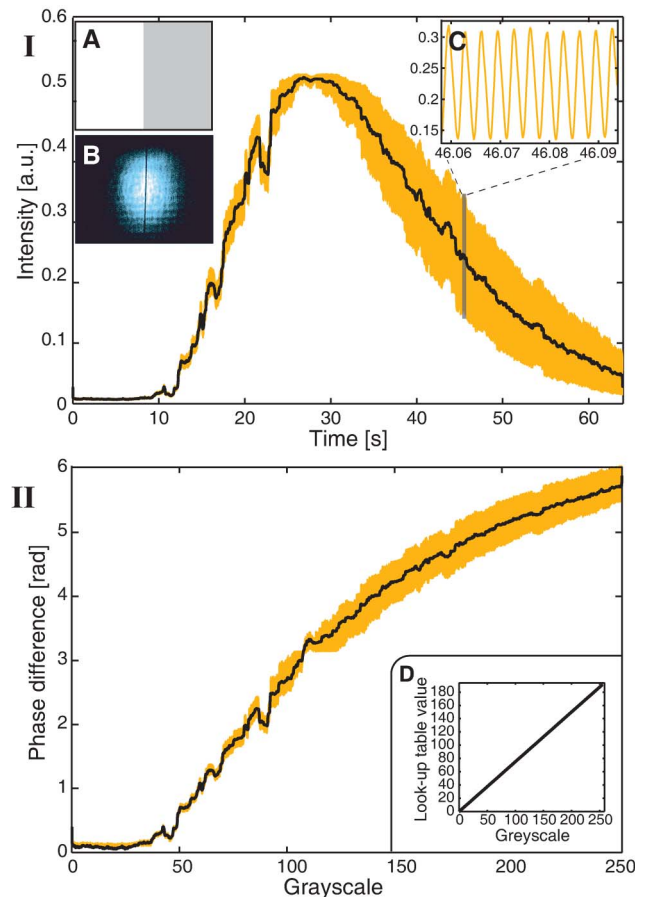


Fig. 3. (Color online) Experimental results obtained with initial SLM configuration and photodiode based detection. I, Evolution of photocurrent as movie is played on SLM. Insets: A, spatial structure of movie encoded on SLM; B, spatial structure of light incident on photodiode; C, phase flicker observable at short time scales. II, Phase response of SLM as a function of gray scale encoded; inset D, LUT utilized by the SLM to convert gray scale to applied voltage across the LCD.

caused by fast phase effects was measurable and was found to have a characteristic time scale of around 300 Hz (Fig. 3, inset C). This flicker is dependent on the depth of phase modulation (gray-scale value) and causes phase fluctuations as large as 1 rad. The noise is caused by the refresh process of the SLM. Each time a pixel is refreshed, the crystal responds to the applied voltage then relaxes as the voltage is removed, causing a periodic fluctuation in the optical thickness [26].

To characterize the stability of the interference pattern, we used a movie with a fixed gray-scale difference and monitored the output intensity for several minutes. The output intensity was stable over this entire time and was not significantly affected by mechanical vibrations, air turbulence, or other factors varying the optical path length. Figure 4 shows a 22 s data sample. Large intensity fluctuations are observed over short time scales; however these are due to the SLM refresh process discussed above rather than instability in the interferometer. Over longer time scales, where SLM refresh noise is small, the interference is remarkably stable. We applied a low-pass filter with a 60 Hz cutoff frequency to the measured intensity data and, after determining P_{\min} and P_{\max} as detailed above, used Eq. (5) to extract the phase difference. The standard deviation of the phase difference was found to be $\sigma = 0.01$ rad, which corresponds to an interferometer relative path length stability of 2 nm. Comparable stability has been achieved in other interferometer-based characterization techniques only by relying on sophisticated active control electronics.

Figure 3, inset B, shows the intensity of light arriving at the photodetector as captured by the CCD camera. Owing to the nature of the Sagnac interferometer this intensity pattern should be symmetric about the \hat{y} axis, with each half carrying identical information about the phase difference. However, some small asymmetries are observed that are due to the misalignment of the center of the optical beams from the \hat{y} axis. This effect only scales the total intensity

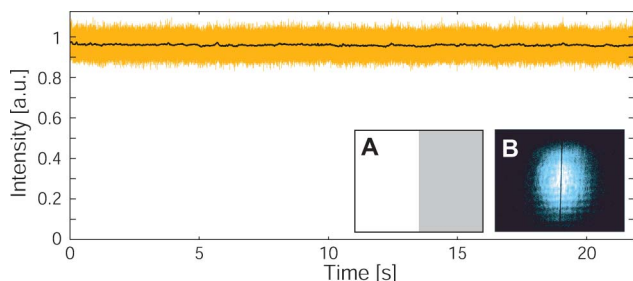


Fig. 4. (Color online) Intensity at Sagnac dark port with fixed nonzero gray-scale value on the right-hand side of the SLM, and zero gray-scale value on the left. Orange (light) trace, unfiltered intensity with fluctuations dominated by fast flicker due to the SLM refresh process; black trace, intensity after low-pass filtering with a 60 Hz cutoff frequency. Insets: A, spatial structure of movie encoded on SLM; B, spatial structure of light incident on photodiode.

observed on each side of the SLM, and therefore has no bearing on the phase characterization.

Notice that the phase response in Fig. 3 is not linear with gray-scale value. This is due to the non-linear response of the SLM to the applied voltage. A linear response is desired in most applications and can be achieved by modifying the LUT of the SLM. As a demonstration, the LUT required to linearize the SLM was determined (Fig. 5, inset C) by using the measured phase response and was applied to the SLM. The phase response of the SLM was then confirmed to be linear, as shown in Fig. 5, part II.

It should be noted that the phase shift determined with our technique is dependent on the optical angle of incidence on the SLM, with larger angles of incidence resulting in longer optical path lengths within the liquid crystal, and consequently larger phase shifts. The phase shift $\Delta\phi$ measured here can be calibrated for an arbitrary angle of incidence θ by using

$$\bar{\Delta\phi}(\theta) = \bar{\Delta\phi}(\theta_{\text{exp}}) \frac{\cos(\theta_{\text{exp}})}{\cos(\theta)},$$

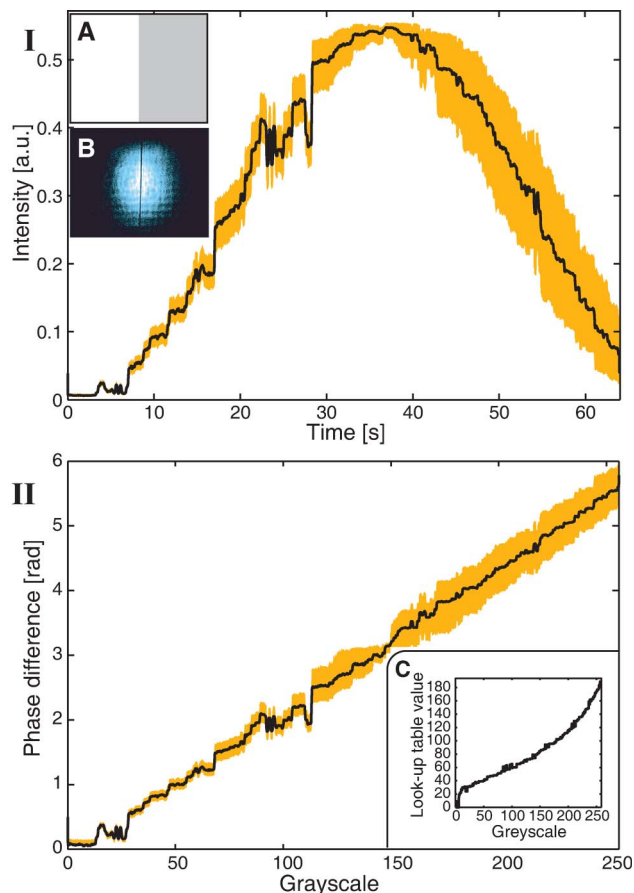


Fig. 5. (Color online) Experimental results obtained with linearized SLM configuration and photodiode based detection. I, Evolution of photocurrent as movie is played on SLM Insets: A, spatial structure of movie encoded on SLM; B, spatial structure of light incident on photodiode. II, Phase response of SLM as a function of gray scale encoded. Inset C, LUT utilized by SLM to convert gray scale to applied voltage across the LCD.

where $\theta_{\text{exp}} = 15^\circ$ is the angle of incidence in our experiment.

C. Characterization of the Transverse Variation in the Phase Response

Most reflective SLMs have a nonuniform phase response over the surface due to inherent curvature of the silicon backplane chip caused by polishing [16,19,26], as well as curvature of the cover glass [18,19]. It is therefore useful to characterize the transverse variation of phase response over the SLM surface. We demonstrate the usefulness of our technique in obtaining this variation by replacing the photodetector with a CCD camera connected to a video capture card (Hauppauge WinTV-HVR-1600) to record the output intensity distribution over the SLM surface. In this case, each pixel on the CCD can be thought of as a single detector; so $\Delta\phi$ now becomes the difference in phase between two pixels at (x,y) and $(-x,y)$ on the SLM screen. As a result of magnifying lenses before the CCD camera, each pixel on the CCD corresponds to an area of 2×2 pixels on the SLM. As before, a movie with one half varying in gray scale from 0 to 255 and one half held at a constant gray scale was used.

Figure 6 shows the intensity profile and phase response from a single pixel of the CCD camera. The phase shows a similar linear response to our previous results using a photodetector rather than a CCD camera, although here the maximum phase shift is greater than 2π , leading to two additional turning points in the observed power, which were accounted for as detailed previously. Characterization of the phase response of such a small area of the SLM would be exceedingly difficult with diffractive techniques and would require active electronic control with other interferometric techniques.

To improve the signal-to-noise ratio, we averaged the intensity over blocks of 8×10 pixels of the CCD camera. We then used the same analysis as in the previous sections to obtain the phase response of the SLM as a function of coordinates over its active surface. The change in gray-scale value needed to achieve a π phase shift was calculated from the slope of the phase response curve and is shown in Fig. 7. To determine the phase response of the entire optically illuminated part of the SLM it was necessary to run two movies ramping the gray scale on the left and the right half of the SLM, respectively; intensity measurements then enabled characterization of the phase response of the corresponding half of the SLM. Some parts of the SLM were too poorly illuminated to obtain reasonable measurements and are grayed out in the figure. The transverse profile indicates that the SLM surface is not optically flat, showing a radial variation. As mentioned above, this is caused by manufacturing limitations such as backplane polishing and the flatness of the cover glass. This is consistent with previous measurements taken with interferometer-based techniques [18]. The data obtained here can be used to calibrate

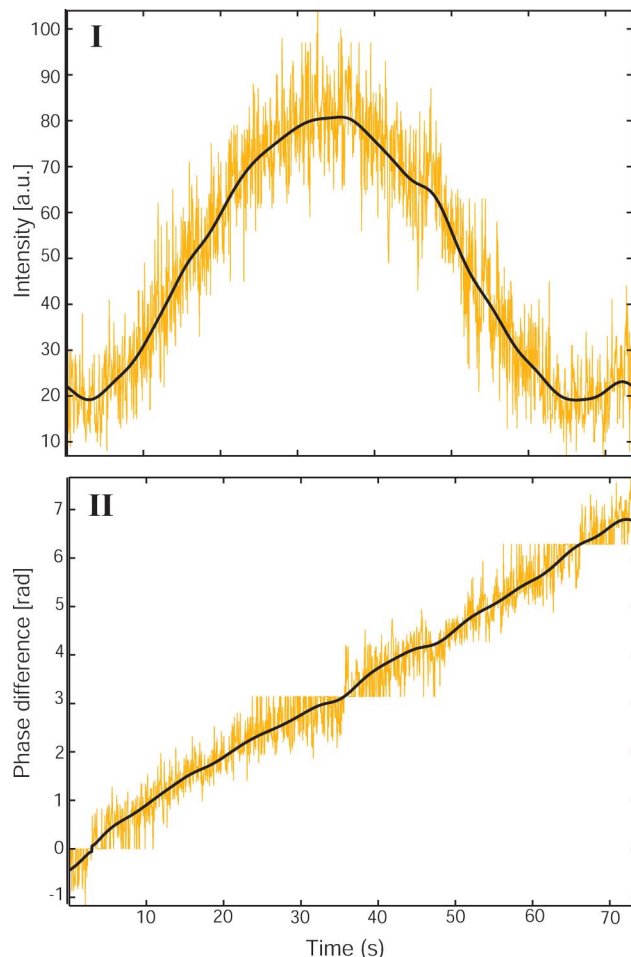


Fig. 6. (Color online) Experimental results obtained for a single pixel with linearized SLM configuration and CCD camera based detection. I, Evolution of incident intensity as movie is played on SLM. II, Phase response of SLM region corresponding to observed pixel as a function of gray scale encoded.

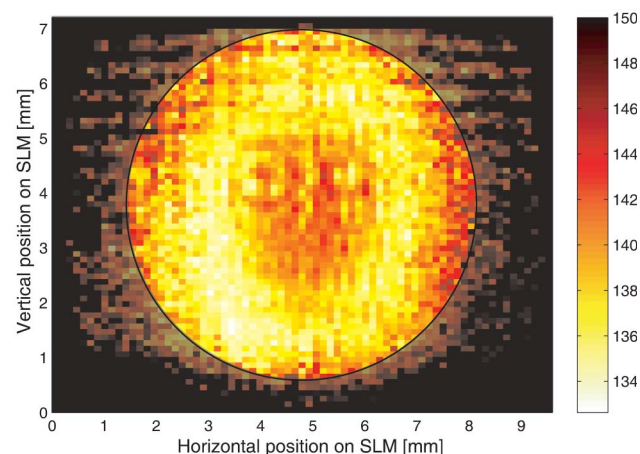


Fig. 7. (Color online) Transverse phase response profile of SLM based on CCD camera measurements. Color bar, change in gray scale needed to achieve a π phase shift. The greyed-out area on the periphery of the figure indicates the region over which light intensities were too low to accurately determine the phase.

the movies used to control the phase, and hence correct for the spatial variation in phase response.

4. Conclusions

We have proposed and demonstrated the use of a Sagnac interferometer to characterize spatially varying phase elements. The method has the accuracy and nonambiguity of interferometric phase element characterization techniques with the self phase-referencing capabilities of diffraction based techniques, combining the advantages of both methods. As a demonstration, the overall phase response of a commercial liquid crystal on silicon SLM was characterized as a function of the gray-scale steerable parameter. The transverse dependence of the phase response of the SLM was also characterized and shown to have a radial variation. The method has significant advantages over other interferometer-based characterization methods, as it is unaffected by environmental factors affecting optical path length such as mechanical vibrations, drift, or air turbulence. It is a simple optical setup that does not require piezo actuators or methods to keep a stable reference. It also has advantages over diffraction-based measurements, as it is simple, is unambiguous, and needs a minimal number of measurements.

This research was supported by the Marsden Fund of New Zealand under the contract 06-UOO-129 PSE, the New Zealand Foundation for Research Science and Technology under the contract NERF-UOOX0703, and the Australian Research Council Discovery Grant DP0985078.

References

1. E. Frumker and Y. Silberberg, "Phase and amplitude pulse shaping with two-dimensional phase-only spatial light modulators," *J. Opt. Soc. Am. B* **24**, 2940–2947 (2007).
2. E. G. van Putten, I. M. Vellekoop, and A. P. Mosk, "Spatial amplitude and phase modulation using commercial twisted nematic LCDs," *Appl. Opt.* **47**, 2076–2081 (2008).
3. A. Bergeron, J. Gauvin, F. Gagnon, D. Gingras, H. H. Arsenaault, and M. Doucet, "Phase calibration and applications of a liquid-crystal spatial light modulator," *Appl. Opt.* **34**, 5133–5139 (1995).
4. J. A. Davis, K. O. Valadéz, and D. M. Cottrell, "Encoding amplitude and phase information onto a binary phase-only spatial light modulator," *Appl. Opt.* **42**, 2003–2008 (2003).
5. C.-S. Guo, Z.-Y. Rong, H.-T. Wang, Y. Wang, and L. Z. Cai, "Phase-shifting with computer-generated holograms written on a spatial light modulator," *Appl. Opt.* **42**, 6975–6979 (2003).
6. J. Davis, E. Carcole, and D. M. Cottrell, "Intensity and phase measurements of nondiffracting beams generated with a magneto-optic spatial light modulator," *Appl. Opt.* **35**, 593–598 (1996).
7. H. J. Tiziani, T. Haist, J. Liesener, M. Reicherter, and L. Seifert, "Applications of SLMs for optical metrology," *Proc. SPIE* **4457**, 72–81 (2001).
8. Y. Takaki and H. Ohzu, "Liquid-crystal active lens: a reconfigurable lens employing a phase modulator," *Opt. Commun.* **126**, 123–134 (1996).
9. M. S. Millán, J. Otón, and E. Pérez-Cabré, "Chromatic compensation of programmable Fresnel lenses," *Opt. Express* **14**, 6226–6242 (2006).
10. A. Márquez, C. Iemmi, J. C. Escalera, J. Campos, S. Ledesma, J. A. Davis, and M. J. Yzuel, "Amplitude apodizers encoded onto Fresnel lenses implemented on a phase-only spatial light modulator," *Appl. Opt.* **40**, 2316–2322 (2001).
11. M. Reicherter, T. Haist, E. U. Wagemann, and H. J. Tiziani, "Optical particle trapping with computer-generated holograms written on a liquid-crystal display," *Opt. Lett.* **24**, 608–610 (1999).
12. E. Schonbrun, R. Piestun, P. Jordan, J. Cooper, K. Wulff, J. Courtial, and M. Padgett, "3D interferometric optical tweezers using a single spatial light modulator," *Opt. Express* **13**, 3777–3786 (2005).
13. E. J. Fernández, B. Považay, B. Hermann, A. Unterhuber, H. Sattmann, P. M. Prieto, R. Leitgeb, P. Ahnelt, P. Artal, and W. Drexler, "Three-dimensional adaptive optics ultrahigh-resolution optical coherence tomography using a liquid crystal spatial light modulator," *Vision Res.* **45**, 3432–3444 (2005).
14. D. McGloin, G. Spalding, H. Melville, W. Sibbett, and K. Dholakia, "Applications of spatial light modulators in atom optics," *Opt. Express* **11**, 158–166 (2003).
15. D. P. Rhodes, D. M. Gherardi, J. Livesey, D. McGloin, H. Melville, T. Freegarde, and K. Dholakia, "Atom guiding along high order Laguerre Gaussian light beams formed by spatial light modulation," *J. Mod. Opt.* **53**, 547–556 (2006).
16. J. Otón, P. Ambs, M. S. Millán, and E. Pérez-Cabré, "Multi-point phase calibration for improved compensation of inherent wavefront distortion in parallel aligned liquid crystal on silicon displays," *Appl. Opt.* **46**, 5667–5679 (2007).
17. J. Reményi, P. Várhegyi, L. Domján, P. Koppa, and E. Lörincz, "Amplitude, phase, and hybrid ternary modulation modes of a twisted-nematic liquid-crystal display at ~ 400 nm," *Appl. Opt.* **42**, 3428–3434 (2003).
18. D. Engström, G. Milewski, J. Bengtsson, and S. Galt, "Diffraction-based determination of the phase modulation for general spatial light modulators," *Appl. Opt.* **45**, 7195–7204 (2006).
19. X. Xun and R. W. Cohn, "Phase calibration of spatially nonuniform spatial light modulators," *Appl. Opt.* **43**, 6400–6406 (2004).
20. T. Kirié, S. Nakadate, and M. Shibuya, "Phase-shifting interferometer based on changing the direction of linear polarization orthogonally," *Appl. Opt.* **47**, 3784–3788 (2008).
21. D. H. Hurley and O. B. Wright, "Detection of ultrafast phenomena by use of a modified Sagnac interferometer," *Opt. Lett.* **24**, 1305–1307 (1999).
22. T. Tachizaki, T. Muroya, O. Matsuda, Y. Sugawara, D. H. Hurley, and O. B. Wright, "Scanning ultrafast Sagnac interferometry for imaging two-dimensional surface wave propagation," *Rev. Sci. Instrum.* **77**, 043713 (2006).
23. H. Sasada and M. Okamoto, "Transverse-mode beam splitter of a light beam and its application to quantum cryptography," *Phys. Rev. A* **68**, 012323 (2003).
24. N. Treps, N. Grosse, W. P. Bowen, M. T. L. Hsu, A. Maitre, C. Fabre, H.-A. Bachor, and P. K. Lam, "Nano-displacement measurements using spatially multimode squeezed light," *J. Opt. B* **6**, S664–S674 (2004).
25. V. Delaubert, N. Treps, C. C. Harb, P. K. Lam, and H.-A. Bachor, "Quantum measurements of spatial conjugate variables: displacement and tilt of a Gaussian beam," *Opt. Lett.* **31**, 1537–1539 (2006).
26. S. Serati, X. Xia, O. Mughal, and A. Linnenberger, "High-resolution phase-only spatial light modulators with sub-millisecond response," *Proc. SPIE* **5106**, 138–145 (2003).